Multiple-Window Spectrogram of Peaks due to Transients in the Electroencephalogram

Maria Hansson*, *Member, IEEE,* and Magnus Lindgren

***Abstract*—In this paper, peak matched multiple windows (PM MW) were used to estimate the spectrogram of the electroencephalogram (EEG). We focussed on the ability to estimate frequency changes, and especially resolving close peaks. A peak of known frequency was evoked in the EEG in a predetermined time interval. The PM MW spectrogram was compared to the commonly used single Hanning window and to weighted overlapped segment averaging in simulations and for real-data. The PM MW were shown to give estimates with good resolution and low variance.**

***Index Terms*—Electroencephalogram, multiple windows, spectrogram, spectrum analysis, spectrum peaks, transient.**

I. Introduction

THE Electroencephalogram (EEG) is the graphic representation of spontaneous brain activity measured with electrodes attached to the scalp. The amplitude is in the range of 10–50 μV and the frequency content of the scalp-recorded EEG is assumed to be below 30 Hz.

The frequency content is usually estimated by successively averaged subspectra from different time epochs. Welch introduced a method where samples were segmented into overlapping sequences and each sequence was windowed, [1]. The algorithm, named weighted overlapped segment averaging (WOSA), has been used in a very large number of applications, including spectrum estimation of EEG. The overlap is often 50%, resulting in small correlation between the averaged subspectra. The drawback of this method is that time resolution is degraded due to the averaging. The variance in the estimate is also large if the frequency properties of the EEG change. Some events of short duration will be difficult to detect and the onset and offset time of those events will be misinterpreted. Such transient frequency changes are often of great interest. In pharmacodynamic studies, for example, it might be crucial to pin-point the start of an arousing effect. Also, event-related changes in the spectrogram are of interest in cognitive studies, [2]. In the time-domain, single-sweep analysis of event-related potentials has been used to describe stimulant effects, [3]. For development of new preparations of drugs with reasonably well-known effects in the frequency domain, such as nicotine, [4], [5], the possibility to pin-point effect onsets is of great interest.

Better estimation of transient events obviously calls for improved time resolution. There are two main approaches to obtain this. The first would be to shorten the window length, which however would cause degraded frequency resolution. The alternative is to reduce the number of windows included in the averaging procedure. The variance then increases during time intervals where changes in the EEG spectrum are small. To reduce the variance estimate, Thomson has proposed the use of multiple windows, [6]. With certain constraints on data, e.g., locally white spectrum, the window-shapes are designed to give uncorrelated subspectra. The advantage of this method is that the fully overlapping windows have different shapes. This method has been used to estimate the multiple window spectrogram for EEG, [7]. However, Walden *et al.*, [8], has shown that for a varying spectrum, e.g., a spectrum that includes peaks, the performance of the Thomson multiple-window method deteriorates due to cross-correlation between the subspectra. When estimating transient peaks in the EEG, the multiple windows should be designed to give uncorrelated spectra for a peaked spectrum, which will give lower variance in the resulting spectrum. In [9], the multiple windows are given as the Karhunen–Loève (KL) basis functions of the covariance matrix of a predefined peaked spectrum. The KL basis functions give uncorrelated spectra at the peak frequency. They are, however, not optimal windows with regard to leakage. To reduce leakage from frequencies outside the main-lobe width, the side-lobes are suppressed using a penalty function outside a predefined frequency interval. The eigenvalue problem for the solution of the KL basis functions is expanded to a generalized eigenvalue problem where the covariance matrix of the penalty function is included. The windows, named Peak Matched Multiple Windows (PM MWs) can be designed for a certain peak shape and frequency resolution. The PM MW spectrogram is used in this paper, with windows designed for the peak shapes of the EEG spectrum. The computational complexity of the new method is about the same as the WOSA algorithm.

Section II defines the spectrogram and the windows used in the analysis. In Section III simulations and variance analysis are presented. Section IV contains examples of real-data and Section V presents the conclusions.

II. Spectrum Analysis

The multiple window spectrogram $\hat{S}(n,k)$ of a real-valued random process $[x_0(0),\ldots,x_0(M_0-1)]^T$, where M_0 is the

Manuscript received September 17, 1999; revised October 26, 2000. *Asterisk indicates corresponding author.*

*M. Hansson is with the Department of Electronscience, Signal Processing Group, Lund University, Box 118, S-221 00 Lund, Sweden (e-mail: Maria.Hansson@tde.lth.se).

M. Lindgren is with the Department of Psychology and the Division of Clinical Neurophysiology, Department of Clinical Neuroscience, Lund University, S-221 00 Lund, Sweden (e-mail: Magnus.Lindgren@knflab.lu.se.

Publisher Item Identifier S 0018-9294(01)01568-3.

total data length, is defined by

$$\hat{S}(n,k)=\sum_{i=1}^{I}\left|\sum_{m=0}^{M-1}x_0(m+nL)h_i(m)e^{-j2\pi\frac{k}{N}m}\right|^2$$
$$k=0,\ldots,N-1;\quad n=0,\ldots,\frac{M_0-M}{L}. \quad (1)$$

It is assumed that the data is stationary for the M samples in $\mathbf{x}=[x_0(nL),\ldots,x_0(M-1+nL)]^T=[x(0),\ldots,x(M-1)]^T$ omitting index n. Equation (1) is a sum of spectrograms obtained by using the data windows $\mathbf{h}_i=[h_i(0),\ldots,h_i(M-1)]^T; i=1,\ldots,I$. The parameter L is the step size of the data and N is the number of points in the discrete Fourier transform.

With one window, $I=1$, the variance of the spectrogram is too large to be useful in frequency analysis, as the variance is $S(n,k)^2$. With more than one window, the variance is reduced if the correlation between the windowed periodograms (subspectra) from the windows $\mathbf{h}_i$ and $\mathbf{h}_j, i\neq j$, is small for all frequency values k. There are different ways to achieve small correlation between the subspectra.

A. WOSA

In the WOSA algorithm, [1], the overlap of the sequences can be varied but it has been shown that 50% overlap is a good choice. The windows are then defined as

$$\mathbf{h}_i=[\underbrace{0,\ldots,0}_{(i-1)\frac{M_w}{2}},\mathbf{h}^T,\ \overbrace{0,\ldots,0}^{M-(i+1)\frac{M_w}{2}}\ ]^T;\quad i=1,\ldots,I \quad (2)$$

where $\mathbf{h}=[h(0),\ldots,h(M_w-1)]^T$ often is a Hanning window and the number of windows I is the largest integer where $I\leq(2M/M_w)-1$. With these windows the data samples $\mathbf{x}$ are divided into overlapping sequences $\mathbf{x}_i=[x((i-1)(M_w/2)),\ldots,x((i+1)(M_w/2)-1)]^T$ and each sequence is windowed with the same data window. It is assumed that the random samples of data give I uncorrelated subspectra which are then averaged.

B. Peak Matched Multiple Windows, PM MW

The PM MW, [9], are designed to give low correlations between subspectra when the spectrum of the random process includes peaks and notches, i.e., a spectrum corresponding to a process with large dynamics. The solution with respect to $\mathbf{h}_i$ is given by the generalized eigenvalue problem

$$\mathbf{R}_B\mathbf{q}_i=\lambda_i\mathbf{R}_Z\mathbf{q}_i;\quad i=1,\ldots,M \quad (3)$$

where the eigenvalues are ordered in decreasing magnitude, $\lambda_1\geq\lambda_2\geq\cdots\geq\lambda_M$. The maximized power is given by the windows $\mathbf{h}_i=\mathbf{q}_i=[q_i(0),\ldots,q_i(M-1)]^T$, corresponding to the I largest eigenvalues. The $(M\times M)$ Toeplitz covariance matrix $\mathbf{R}_B$ has the elements $r_B(l)=r_{x_d}(l)*B\,\mathrm{sinc}(Bl), 0\leq|l|\leq M-1$, where $r_{x_d}(l)$ is the covariance function of a desired peaked spectrum process $x_d(n), \mathrm{sinc}(u)=\sin(\pi u)/\pi u$, and $*$ denotes the convolution operator. The choice of desired peaked spectrum corresponding to $x_d(n)$ is

$$S_{x_d}(f)=e^{\frac{-2C|f|}{10B\log_{10}(e)}};\quad |f|\leq 1/2 \quad (4)$$

which gives the peak $S_{x_d}(0)=1$ (0 dB) and $S_{x_d}(|B/2|)=-C$ dB. The covariance matrix $\mathbf{R}_Z=\mathbf{R}_G$ corresponds to the penalty frequency function

$$S_G(f)=\begin{cases}10^{\frac{G}{10}}, & B/2<|f|\leq 1/2\\ 1, & -B/2\leq f\leq B/2\end{cases} \quad (5)$$

which is used to reduce the leakage from the side-lobes outside the frequency interval $|f|>B/2$, and where the value of G indicates the suppression factor. Minimization of mean square error (mse) is fulfilled if $\mathbf{h}_i$ is weighted with $\sqrt{\lambda_i}$, i.e., $\mathbf{h}_i=\sqrt{(\lambda_i/\sum_{i=1}^{I}\lambda_i)}\mathbf{q}_i$, which is used in this paper, [10].

The parameters of the PM MW are not sensitive to the shape of the spectrum. However, for an optimal detection of peaks the windows should be designed to fit the application. An average of spectra can be used to select the parameter C to obtain a good fit between the desired spectrum $S_{x_d}(f)$ and the original spectrum. In order to minimize leakage from frequencies of large power, the bandwidth B should not be too wide. For spectra with large power variations in small frequency intervals 2 Hz is recommended. For smoother spectra the bandwidth can be three or four times larger. The choice of the suppression factor G outside this bandwidth is determined by the magnitude of the power variations in the spectrum. Usually $G=$ 10–30 dB is recommended. The combination of parameters will decide the number of windows, which in turn influences the variance properties of the algorithm. Larger bandwidth B and smaller suppression factor G will increase the number of windows, resulting in smaller variance.

To illustrate the frequency shape of the different choices of parameters, a few examples are given in Fig. 1. The window spectra are given as $S_w(f)=\sum_{i=1}^{I}|H_i(f)|^2$ where $H_i(f)$ is the Fourier transform of the window $\mathbf{h}_i$. The frequency scale is given in hertz for the sampling frequency $F_s=64$ Hz. In Fig. 1(a) the PM MW spectra are depicted for $C=30$ dB and different examples of the suppression factor G and bandwidth B. The solid and dashed lines represent windows where the suppression factors are $G=20$ dB and $G=0$ dB, respectively. The shape of the spectrum is peaked which will contribute to the resolving of close peaks. The dash-dotted line is the window spectrum with a main-lobe width $B=2/64$. This window spectrum has a shape similar to the Hanning window but the number of windows is $I=3$. This will reduce the variance in the spectrum estimate compared to the single Hanning window (dotted line). In Fig. 1(b), the dashed line represents the window spectrum of the WOSA for $I=3$ windows. The main-lobe width is 4 Hz and the shape of the spectrum will not help resolving close peaks. With fewer windows (solid line) or longer total window (dash-dotted line), the main-lobe width will be reduced.

III. Simulations

The purpose of this section is to show that the PM MWs can increase the time resolution further with preserved variance properties, compared to the WOSA algorithm. The simulated signal is created as a time-variable autoregressive moving average (ARMA)-process where the parameters of the process change at certain time points. The ARMA-process is defined as shown in (6) at the bottom of the next page, where

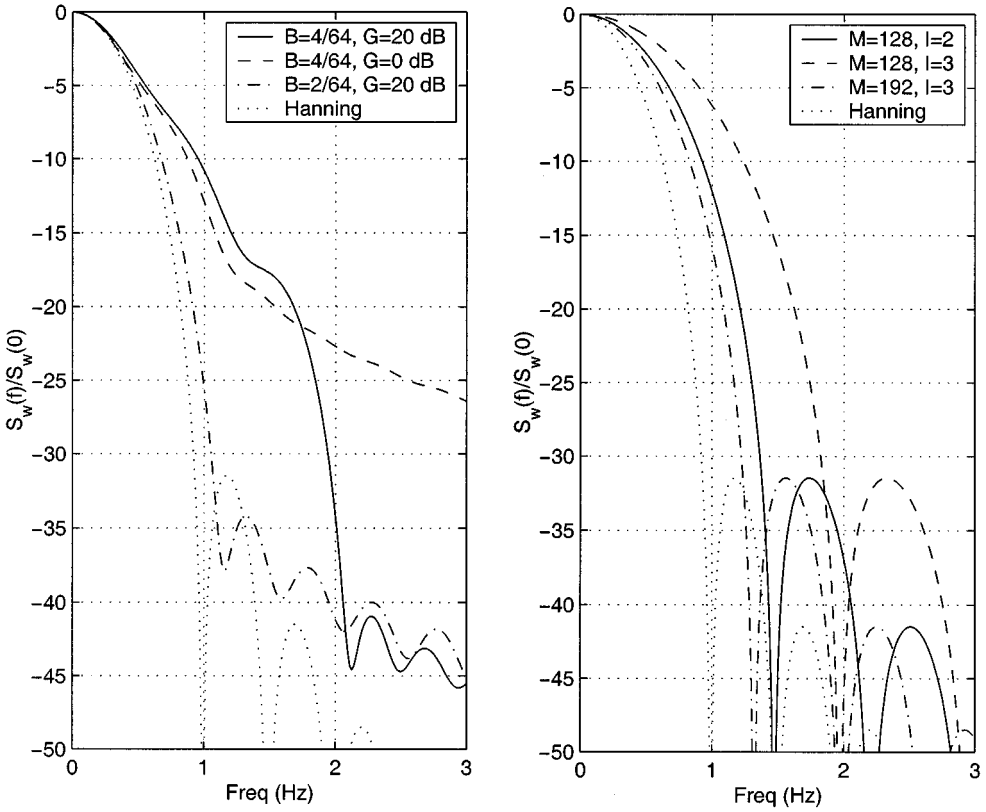

(a) (b)

Fig. 1. (a) Window spectrum, (solid line = PM MW, $M = 128$, $I = 4$, $B = 4/64$, $C = 30$, $G = 20$; dashed line}= PM MW, $M = 128$, $I = 4$, $B = 4/64$, $C = 30$, $G = 0$; dash-dotted line} = PM MW, $M = 128$, $I = 3$, $B = 2/64$, $C = 30$, $G = 20$; dotted line = Hanning window, $M = 128$); (b) Window spectrum, solid line}= WOSA, $M = 128$, $I = 2$; dashed line = WOSA, $M = 128$, I =3; dash-dotted line = WOSA, $M = 192$, $I = 3$; dotted line = Hanning window, $M = 128$).

TABLE I
PARAMETERS OF THE SIMULATED TIME-VARIABLE ARMA-PROCESS

i	$\alpha_1(i)$	$f_1^\alpha(i)$	$\beta_1(i)$	$f_1^\beta(i)$	$\alpha_2(i)$	$f_2^\alpha(i)$	$\beta_2(i)$	$f_2^\beta(i)$	$\alpha_3(i)$	$f_3^\alpha(i)$	$\beta_3(i)$	$f_3^\beta(i)$
1,2	0.93	± 1	0.5	± 2	0.94	± 2	0.92	± 3	0.93	± 1	0.5	± 2
3,4	0.93	± 4	0.5	± 6	0.93	± 4	0.8	± 6	0.93	± 4	0.5	± 6
5,6	0.93	± 7	0.5	± 8	0.97	± 9	0.95	± 9.6	0.93	± 7	0.5	± 8
7,8	0.95	± 10.2	0.5	± 14	0.97	± 10.2	0.8	± 14	0.95	± 10.2	0.5	± 14

$F_s = 64$ Hz and K_q is a normalization factor which gives constant total power. The parameters are presented in Table I for the three different time epochs, q =1, 2, 3, where the different processes are active during the time periods $t = -3$ s to 0 s, $t = 0$ s to 2 s and $t = 2$ s to 7 s, respectively. Notice that $H_1(z) = H_3(z)$. An example of a simulated signal is shown in Fig. 2(a). Fig. 2(b)–(d) shows the amplitude spectra of the infinite impulse response-filters. Fig. 2(b) is dominated by delta and theta activity, an EEG from a slightly drowsy subject with closed eyes. Fig. 2(c) shows a spectrum where the alpha activity has increased and a 9-Hz flicker has been introduced. This gives two close peaks, which call for good frequency resolution properties of the spectrum estimation algorithms. In Fig. 2(d), the spectrum is again more dominated by theta and the alpha peak is reduced. The introduced 9-Hz signal is not present in this time interval.

$$H_q(z) = \frac{1}{K_q} \frac{(1-0.5z^{-1})(1+z^{-1}) \prod_{i=1}^{4} \left(1 - 2\beta_q(i)\cos\left(2\pi \frac{f_q^\beta(i)}{F_s}\right) z^{-1} + \beta_q^2(i) z^{-2}\right)}{\prod_{i=1}^{4} \left(1 - 2\alpha_q(i)\cos\left(2\pi \frac{f_q^\alpha(i)}{F_s}\right) z^{-1} + \alpha_q^2(i) z^{-2}\right)} \tag{6}$$

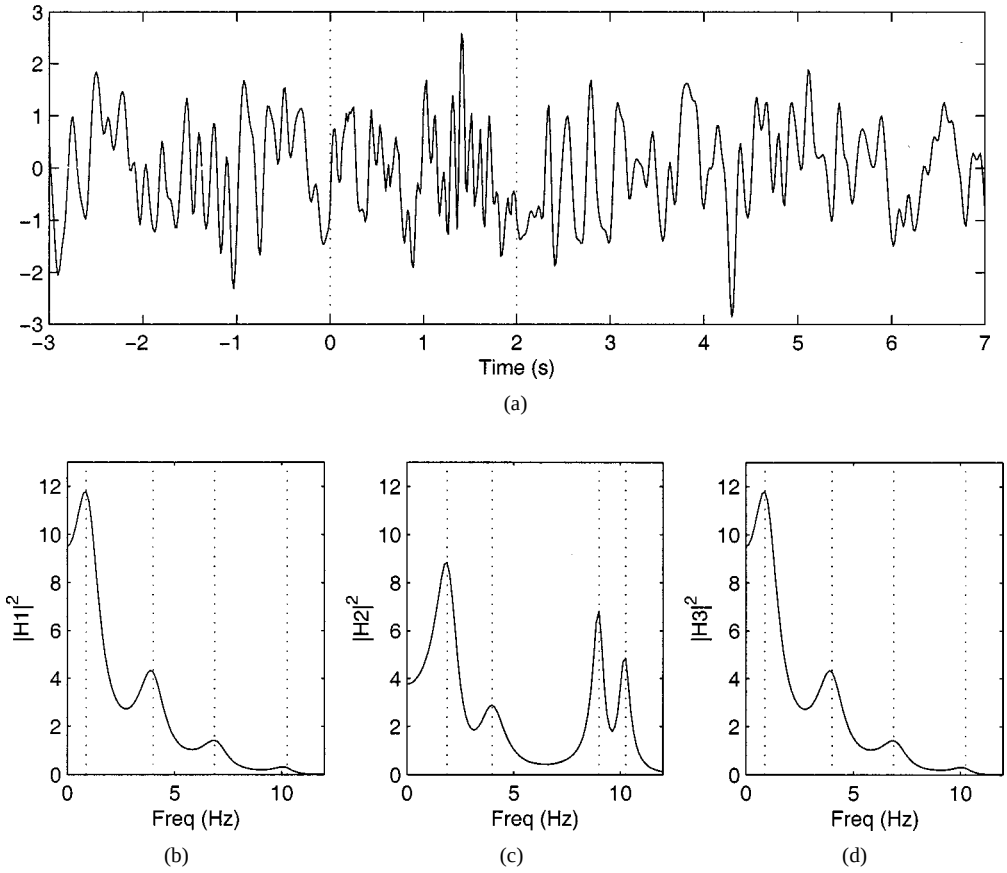

(a) (b) (c) (d)

Fig. 2. Simulated data where the process parameters change at $t = 0$ s and $t = 2$ s; (a) An example of a data sequence; (b) ARMA1 ($t = -3$–0 s); (c) ARMA2 ($t = 0$–2 s); (d) ARMA3 ($t = 2$–7 s).

A. Calculation of Bias and Variance

The bias and variance can be calculated since the true ARMA-spectrum is known. A comparable measure for different frequencies is obtained if the bias and variance are divided by $E[\hat{S}(n,k)]$, and $E[\hat{S}(n,k)]^2$, respectively. This implies that small valued estimates are related in the same way as large valued estimates. Bias is defined as

$$\text{Bias } \hat{S}(n,k) = \frac{E[\hat{S}(n,k)] - S(n,k)}{E[\hat{S}(n,k)]} \tag{7}$$

where the expected value of the spectrogram estimate is calculated to be

$$\begin{aligned} E[\hat{S}(n,k)] &= E\left[\sum_{i=1}^{I} \mathbf{h}_i^T \mathbf{\Phi}^H(k)\mathbf{x}\mathbf{x}^T\mathbf{\Phi}(k)\mathbf{h}_i\right] \\ &= \sum_{i=1}^{I} \mathbf{h}_i^T \mathbf{\Phi}^H(k)\mathbf{R}_x\mathbf{\Phi}(k)\mathbf{h}_i. \end{aligned} \tag{8}$$

In (8), $\mathbf{\Phi}(k) = \text{diag}[1, e^{-j2\pi(k/N)}, \ldots, e^{-j2\pi(M-1)(k/N)}]$ is the Fourier transform matrix. The variance of the spectrogram estimate is given by all combinations of the different subspectra covariances

$$\text{Variance}\,\hat{S}(n,k) = \frac{\sum_{j=1}^{I}\sum_{i=1}^{I} \text{cov}(\hat{S}_i(n,k)\hat{S}_j(n,k))}{E[\hat{S}(n,k)]^2}. \tag{9}$$

Denoting $\mathbf{h}_i^T\mathbf{\Phi}^H(k)\mathbf{x} = A_i$ and assuming $\mathbf{x}$ to be Gaussian gives the covariance as

$$\begin{aligned} &\text{cov}(\hat{S}_i(k)\hat{S}_j(k)) \\ &\quad = \text{cov}\left(A_iA_i^HA_jA_j^H\right) \\ &\quad = E\left[A_i^HA_iA_jA_j^H\right] - E\left[A_i^HA_i\right]E\left[A_jA_j^H\right] \\ &\quad = E\left[A_i^HA_j\right]E\left[A_iA_j^H\right] + E\left[A_i^HA_j^H\right]E\left[A_iA_j\right] \\ &\quad = \left|\mathbf{h}_i^T\mathbf{\Phi}^H(k)\mathbf{R}_x\mathbf{\Phi}(k)\mathbf{h}_j\right|^2 + \left|\mathbf{h}_i^T\mathbf{\Phi}(k)\mathbf{R}_x\mathbf{\Phi}(k)\mathbf{h}_j\right|^2 \end{aligned} \tag{10}$$

according to Walden *et al.*, [8].

The covariance matrix $\mathbf{R}_x$ will be symmetric and Toeplitz in the stationary case, i.e., when the data samples $\mathbf{x}$ is the result of only one process. In the nonstationary case

$$\mathbf{x} = [\underbrace{x(0), \ldots, x(L_s-1)}_{\mathbf{x}^a}, \underbrace{x(L_s), \ldots, x(M-1)}_{\mathbf{x}^b}]^T \tag{11}$$

where $\mathbf{x}^a$ and $\mathbf{x}^b$ is resulting from different processes, the matrix $\mathbf{R}_x$ is defined by the real-valued matrix

$$\mathbf{R}_x = \begin{bmatrix} \mathbf{R}_{x_ax_a} & \mathbf{R}_{x_ax_b} \\ \mathbf{R}_{x_bx_a} & \mathbf{R}_{x_bx_b} \end{bmatrix} \tag{12}$$

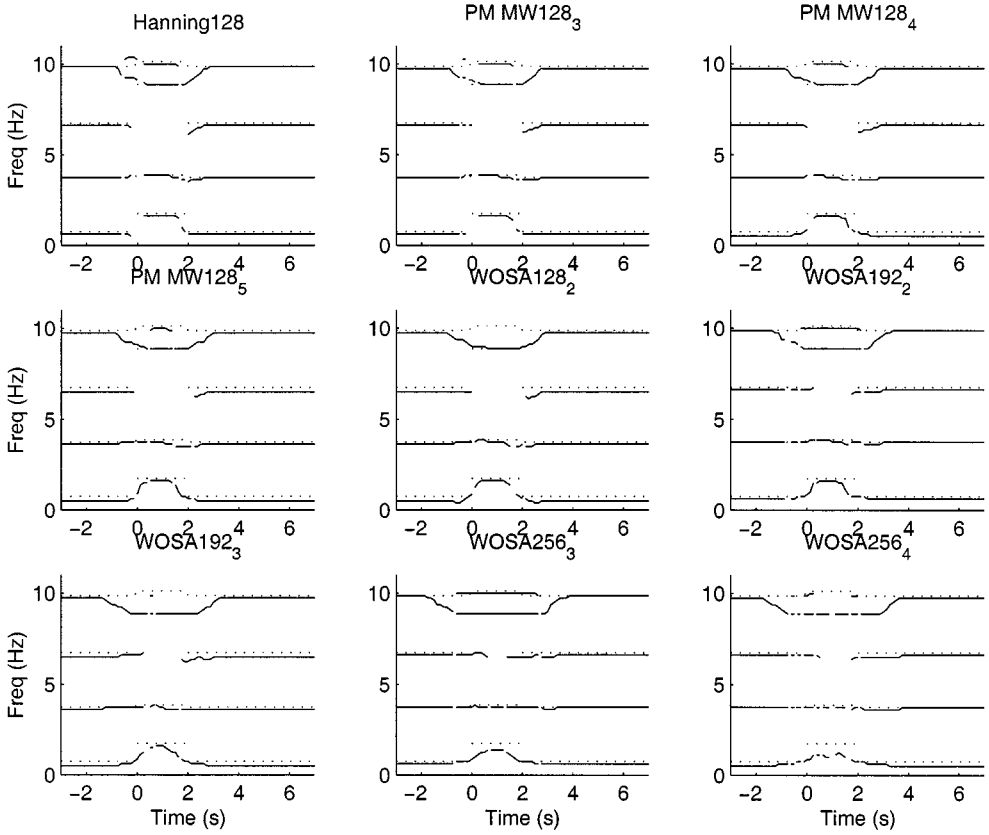

Fig. 3. Peaks of the expected values of the spectrogram for different methods, (solid line $= E[\hat{S}(n,k)]$, dotted line $= S(n,k)$).

which is a non-Toeplitz, symmetric matrix including the $(L_s \times L_s)$ and $(M-L_s \times M-L_s)$ Toeplitz covariance matrices $\mathbf{R}_{x_a x_a}$ and $\mathbf{R}_{x_b x_b}$, and the cross-covariance matrices

$$\mathbf{R}_{x_a x_b} = \begin{bmatrix} r_{x_a x_b}(L_s) & \cdots & r_{x_a x_b}(M-1) \\ r_{x_a x_b}(L_s-1) & & r_{x_a x_b}(M-2) \\ \vdots & & \vdots \\ r_{x_a x_b}(1) & \cdots & r_{x_a x_b}(M-L_s) \end{bmatrix} \quad (13)$$

and $\mathbf{R}_{x_b x_a} = \mathbf{R}^T_{x_a x_b}$. The transient effects in the changes of processes are assumed to be small.

B. Evaluation

The evaluated methods should be able to resolve all the peaks of the spectra and especially the alpha peak and the introduced signal at 9 Hz, which are quite close to one another.

For the PM MWs the desired spectrum parameter $C = 30$ and the penalty function parameter $G = 20$ dB. The length of the windows is $N = 128$ which corresponds to 2 s of data with the sample frequency $F_s = 64$ Hz. Three different predefined peak shapes are tested by defining $B =$ 4/64, 3/64, and 2/64 which gives a number of $I = 5$, 4, and 3 multiple windows, respectively. The methods are named PM MW128$_5$, PM MW128$_4$ and PM MW128$_3$.

For the WOSA method, different total window lengths M are used as well as different numbers of windows I. The combinations are named WOSAM_I. In the case of WOSA192$_2$ and WOSA256$_3$ it is interesting to note that the length of the Hanning windows is $M_w = 128$ in both cases, which implies that the resolution of these two algorithms is the same as the single Hanning window, Hanning128.

The resolutions of the different methods are compared in Fig. 3. The dotted lines represent the true frequency location of the peaks of the spectra in Fig. 2. The four peaks of the process ARMA 1 are plotted as dotted lines for $t < 0$ s. Between 0 and 2 s the dotted lines are changed to the pattern of the process ARMA 2 which has two close peaks at 10 Hz. These two peaks are represented as the two parallell lines at 10 Hz between 0 and 2 s. For $t > 2$ s the spectrum peaks are located as for the process ARMA 3. The solid lines represent the frequency location of the peak values of the different methods. The peak values are found from the calculation of the expected values, (8), and by searching the zero-crossing of the difference $E[\hat{S}(n,k)] - E[\hat{S}(n,k-1)]$ for each time sample n.

The Hanning128 has the resolution needed to estimate the close peaks of ARMA 2 which is active during the time period 0–2 s. The PM MW methods have about the same performance as Hanning128 and it can be concluded that the PM MW method is not sensitive to choice of parameters as long as the desired peaked spectrum is reasonably similar to a total average EEG spectrum. The WOSA128$_2$, WOSA192$_3$, and WOSA256$_4$ all fail in resolving the peaks at 9 Hz and 10.2 Hz. The reason is that the windows are too wide and the two peaks become one. The WOSA192$_2$ and WOSA256$_3$ have the same performance as Hanning128 for the stationary case. The total window length is 3 and 4 s, respectively, instead of 2 s, which means degraded time resolution. This is seen as certain frequencies last too long and start too early, especially for the WOSA256$_3$. The ability

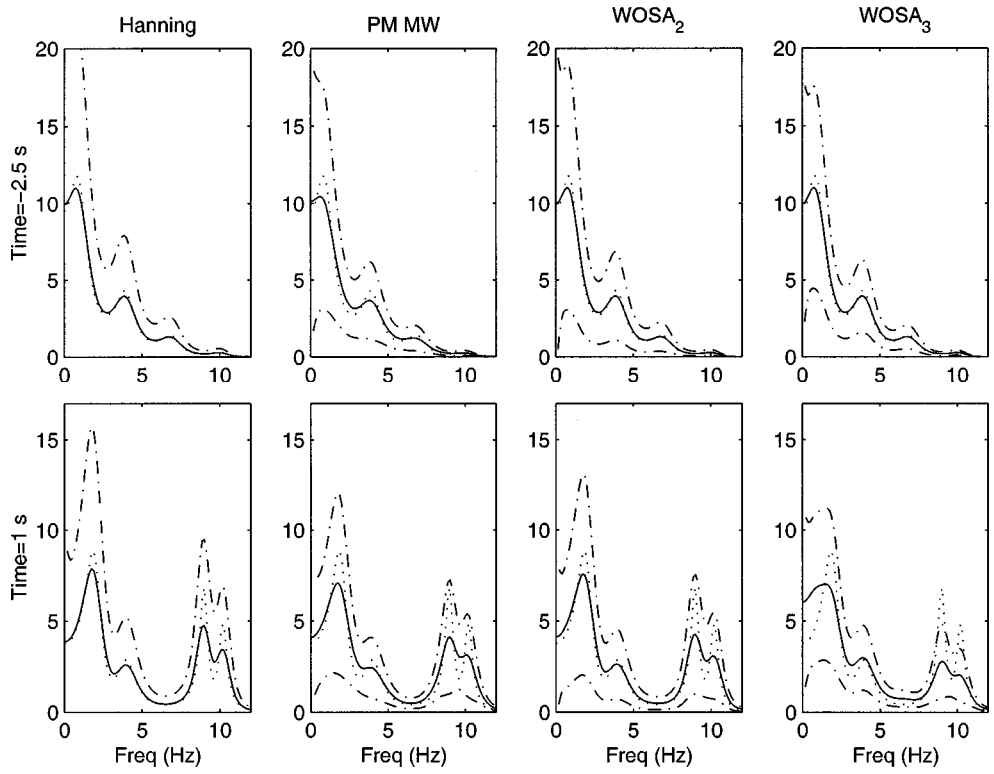

Fig. 4. Calculated expected values of spectrogram estimates for different methods for two time points: Time $= -2.5$ s (upper row) and 1 s (lower row), (solid line $= E[\hat{S}(n,k)]$, dash-dotted line $= E[\hat{S}(n,k)] \pm \mathrm{std}[\hat{S}(n,k)]$, dotted line $= S(n,k)$).

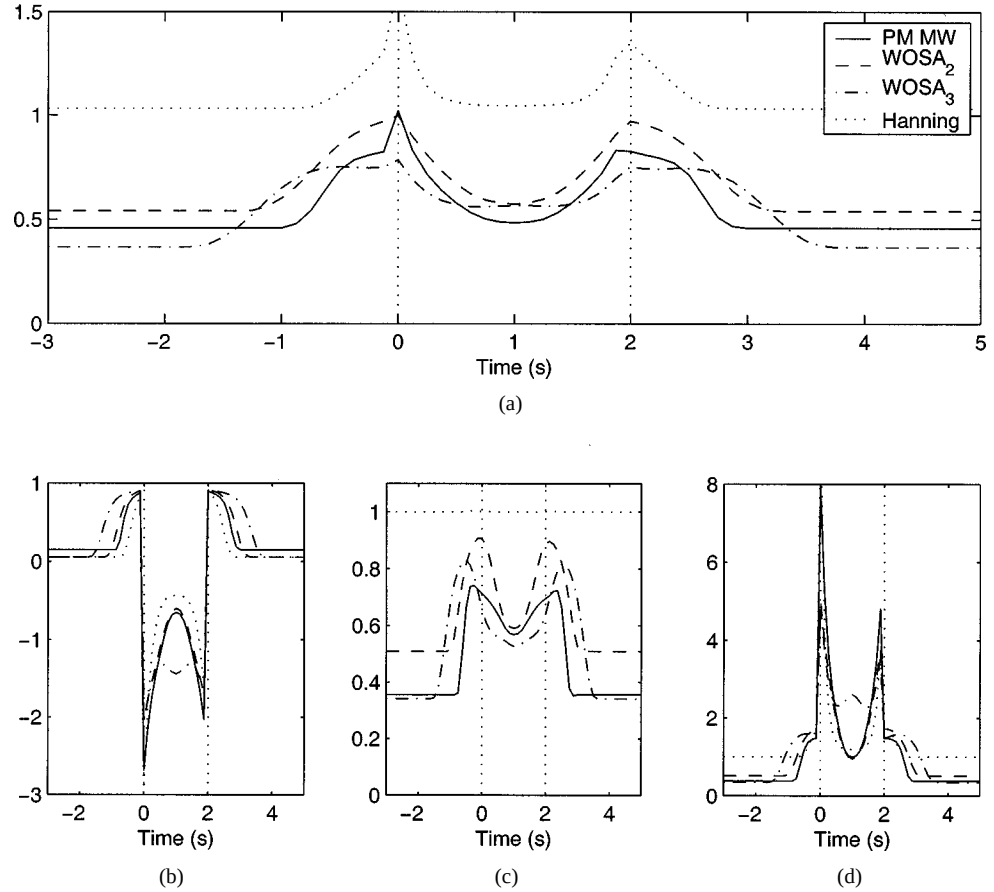

Fig. 5. (a) Average of MSE for $f = 0$–12 Hz; (b) normalized bias; (c) normalized variance; (d) normalized mse, (solid line $=$ PM MW, dashed line $= \mathrm{WOSA}_2$, dashed-dotted line $= \mathrm{WOSA}_3$, dotted line $=$ Hanning window).

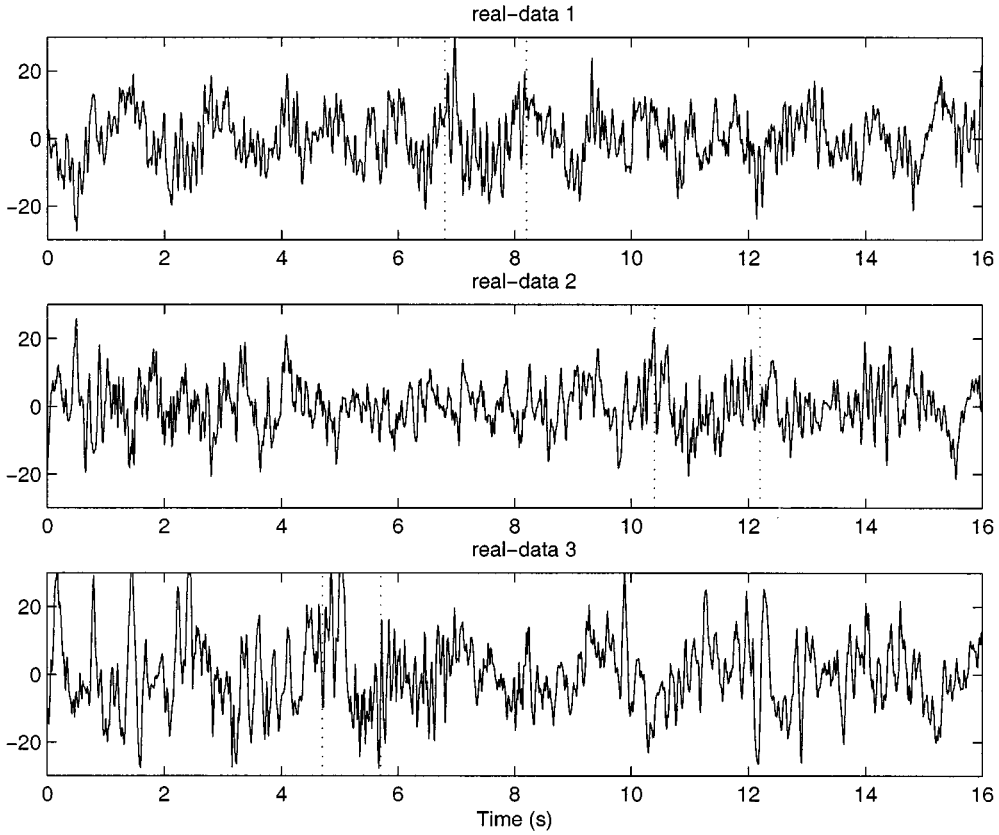

Fig. 6. Real-data examples from channel Pz where a 9-Hz flickering light is introduced during the time interval between the dotted lines.

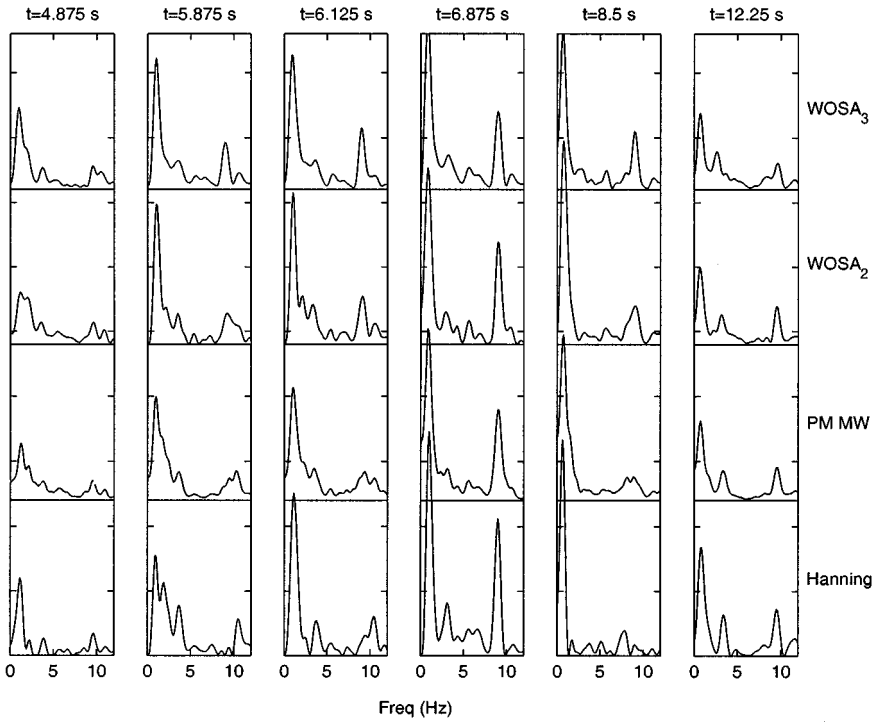

Fig. 7. Spectrum at different time points of real-data 1.

to track a changing frequency will also be impaired, e.g., 1 Hz changing to 2 Hz and back again. If the length M of the data included in the WOSA is increased beyond 4 s to enlarge the number of windows I in the estimate with preserved resolution, the algorithm will no longer be able to track a short frequency change, e.g., 1 Hz to 2 Hz.

From now on we study four of the methods, which are able to resolve the close peaks at 9 Hz and 10.2 Hz and which have

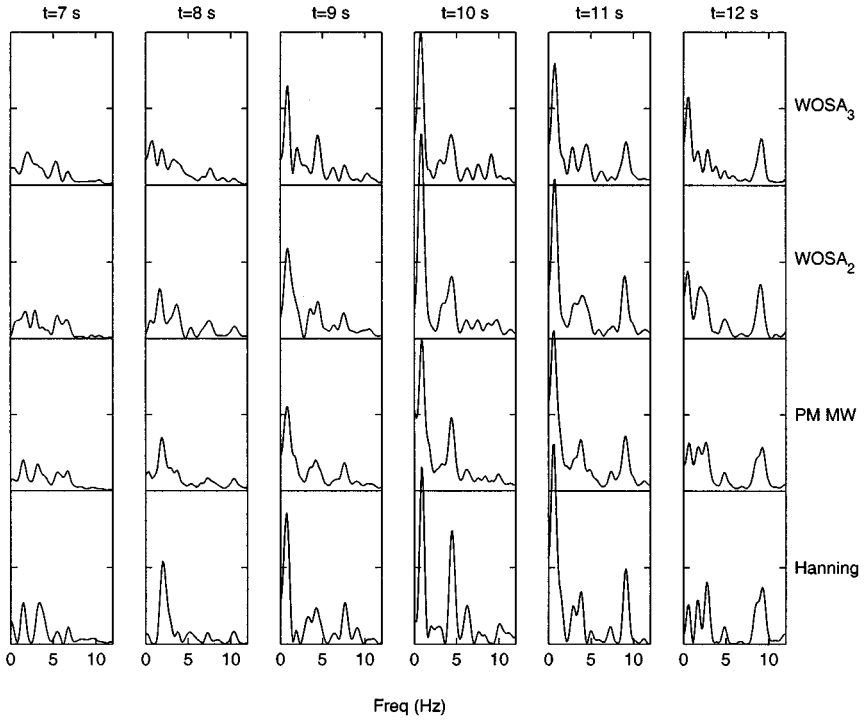

Fig. 8. Spectrum at different time points of real-data 2.

sufficient time resolution to track the change from 1 Hz to 2 Hz. For reasons of simplicity we name them as follows: The Hanning128 is Hanning, PM $MW128_5$ is PM MW, $WOSA192_2$ is $WOSA_2$ and $WOSA256_3$ is $WOSA_3$. In Fig. 4, the expected value is depicted as the solid line for the four methods and for two time points: Time $= -2.5$ and 1 s. The expected value plus and minus one standard deviation is depicted as the dash-dotted line, and the true spectrogram is the dotted line. The expected values and standard deviations of the PM MW, $WOSA_2$ and $WOSA_3$ are similar, but for the Hanning spectrogram the standard deviation is $E[\hat{S}(n,k)]$, which makes the lower bound equal to zero and the upper bound $2E[\hat{S}(n,k)]$. The first case in the upper row is when the low-frequency dominant spectrogram is stationary. The second case in the lower row is in the middle of the time period 0–2 s when the 9-Hz flicker is present. These snap-shots in time of the spectrogram show that the PM MW have a shape similar to those of the Hanning window, $WOSA_2$ and $WOSA_3$. The variance is somewhere between the variances of $WOSA_2$ and $WOSA_3$. The time resolution for the PM MW $(M = 128)$ is, however, better than for the $WOSA_2$ $(M = 192)$ and $WOSA_3$ $(M = 256)$.

The mses are normalized with the squared expected value for every frequency value. The average over the frequencies 0–12 Hz of this measure is shown in Fig. 5(a). The $WOSA_3$ method (dash-dotted line) has the lowest value for the stationary part of the signal. The window length is however 4 s, which makes the transient start shortly after -2 s and end close to 4 s. The solid line is the PM MW method, which has a slightly larger mse in the stationary region, but the transient is shorter as the window length is 2 s, which is the same as that given by the Hanning window (dotted line) and shorter than both the $WOSA_2$ (3-s average) and the $WOSA_3$ (4-s average).

In Fig. 5(b)–(d), the normalized bias, variance, and mse of the peak frequency 9 Hz is plotted for the four different methods. In the stationary part the PM MW method (solid line) has a larger bias than the Hanning window (dotted line), $WOSA_2$ (dashed line) and $WOSA_3$ (dash-dotted line), but as the variance is low, the mse of the PM MW method is about the same as for the $WOSA_2$ and $WOSA_3$ methods.

IV. Real Data Examples

To show the performance for real-data, three EEG samples from channel Pz were studied. In all three samples, a 9-Hz flickering light (Grass Photic stimulator Model PS22C) was introduced at different time points. The light stimulation lasted between 1 and 2 s. Data was recorded using a Neuroscan system with a digital amplifier (SYNAMP 5080, Neuro Scan, Inc.). Amplifier bandpass settings were 0.3 and 50 Hz. The sample rate was 256 Hz. EEG was converted into 2.0-s epochs, and subsequently exported from the Neuroscan system for further analysis. The data was then downsampled to a sample rate of 64 Hz.

The subject was supine with closed eyes on a bed in a silent laboratory. Ambient light was dimmed. At irregular intervals, flickering light was flashed at the subject from a distance of approximately 1 m.

The data samples are seen in Fig. 6.

The four methods, PM MW, $WOSA_2$, $WOSA_3$, and Hanning window were tested on the real-data sequences and the spectrum estimates are depicted for different time points. The idea of depicting the result of these four methods is to show that the PM MW behave similarly to the $WOSA_2$ and $WOSA_3$ in the stationary time intervals. In the transient time intervals, when

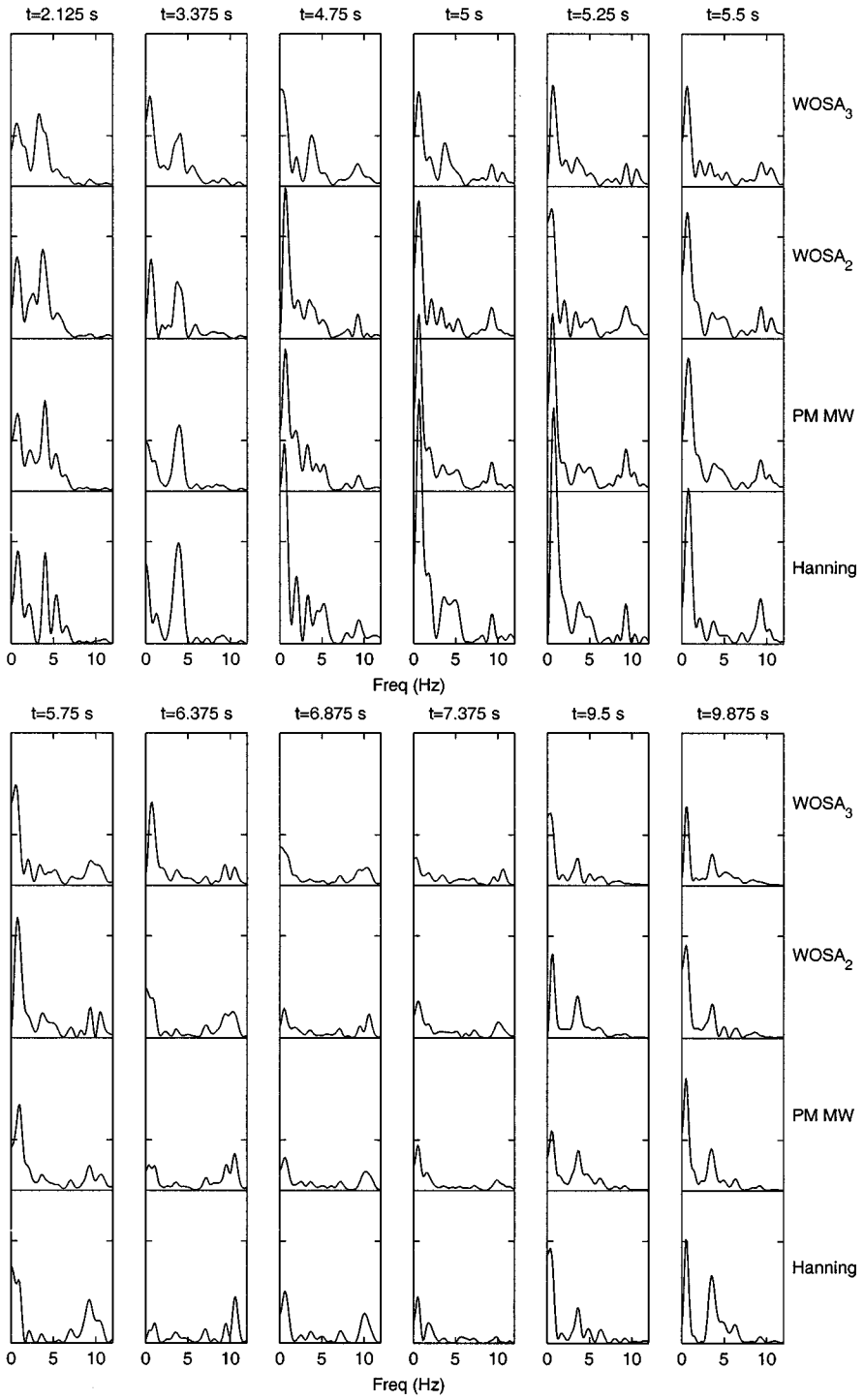

Fig. 9. Spectrum at different time points of real-data 3.

the flickering light was flashed, the goal is to show that the PM MW behave similarly to the Hanning window from a time resolution viewpoint. In Fig. 7, the result of the first sequence is shown. The Hanning window has spectrum estimates with large variations over the frequency scale. This is caused by the large variance in the method and is not relevant to the transient frequency changes. At time points $t = 4.875$ and $t = 12.25$ s, the three methods, PM MW, WOSA_2, and WOSA_3, have similar spectra which confirm the reliability of these three methods in stationary intervals. The 9-Hz flicker starts at 6.8 s, which means that the frequency values at 9 Hz should be fairly small in the interval preceding that time-point. This is true for the Hanning window and the PM MW method, which is to be expected as these methods have a better time resolution than the WOSA_2 and WOSA_3. The WOSA_3 shows a 9-Hz peak already at $t = 5.875$ s and the WOSA_2 at $t = 6.125$ s. This is not a desirable result. The same behavior is seen at $t = 8.5$ s where both WOSA_2 and WOSA_3 show a 9-Hz peak.

In the second data example, the 9-Hz flicker starts at $t = 10.4$ s and stops at $t = 12.2$ s. The result is seen in Fig. 8 where

time samples from $t = 7$–12 s are shown. From $t = 7$ s to 11 s a rise of delta activity is seen. All methods are comparable for this slow change over time. A faster change in theta activity at about 4 Hz can also be seen. This change does not show as clearly for the WOSA_3 as it does for the other methods. The drawback of the WOSA_3 is that it cannot detect fast changes with time. Theta activity falls back again when the flickering starts at $t = 10.4$ s. The 9 Hz is clearly visible at $t = 11$ s for all methods.

In the third example, the 9-Hz flickers starts at $t = 4.7$ s and stops at $t = 5.7$ s. The spectrum at $t = 2.125$ s and $t = 3.375$ s, has similar appearance for all methods. This is a stationary time interval and all methods are similar from a time resolution viewpoint. The largest difference is seen for the Hanning window as the variation over frequencies are large. As these changes are caused by the large variance of the method, these spectrum changes are not relevant. The 9-Hz peak is visible in the results of all methods at $t = 4.75$ s and is no longer seen for the Hanning window and the PM MW at $t = 6.875$ s, which is to be expected as half the window length is 1 second. For the WOSA methods it takes about 1 s more before the peak is gone. It is also interesting that the start of the flicker initiates alpha activity. This is seen in Fig. 9 especially around $t = 5.5$ s where a double peak at 9 and 10 Hz is seen more or less clearly for the different methods. The alpha activity lasts somewhat longer than the introduced 9 Hz, then the spectrum is again dominated by delta and theta activity.

V. Conclusion

The ability to estimate transient peaks in the EEG has been investigated using the multiple window spectrogram. The multiple windows were designed to give uncorrelated spectra at the peak frequencies which result in low variance estimates. The proposed method is not very sensitive to the choice of parameters as long as the desired peaked spectrum used for the window estimation has a shape similar to the average EEG spectrum. For the purposes of this paper, a frequency resolution of 1–2 Hz was desired. The bandwidth of the desired spectrum was chosen accordingly. When a lower resolution is sufficient, a wider bandwidth can be chosen. The larger number of windows will result in a reduced variance. The time- and frequency-resolution of the windows can be designed for specific applications. Specific hypotheses about frequency changes in given time segments can thus be tested through dedicated windows. For instance, in nicotine studies it can be of interest to study changes in the sensitive alpha 2 band (10–12 Hz), and corresponding windows can be applied to EEG data. The different spectrum shapes are robust, which means that they can be used across subjects in a clinical study. Simulations show that the PM MWs give smaller variance and better time resolution than the commonly used single Hanning window and the WOSA method for the same frequency resolution. The real-data examples confirm that the proposed method could be used in applications where transient peaks are present in the EEG and where both time and frequency resolution is important.

Acknowledgment

The authors would like to thank laboratory technician A. Walfisz for expert help with the electrophysiological recording. They would also like to thank R. Sassani and S. Pourtorab for working on this project in their master thesis.

References

[1] P. D. Welch, "The use of fast Fourier transform for the estimation of power spectra: A method based on time averaging over short, modified periodograms," *IEEE Trans. Audio Electroacoust.*, vol. AU-15, pp. 70–73, June 1967.

[2] W. Klimesch, M. Doppelmayr, H. Schimke, and B. Ripper, "Theta synchronization and alpha desynchronization in a memory task," *Psychophysiology*, no. 34, pp. 169–176, 1997.

[3] R. Halliday, H. Naylor, D. Brandeis, E. Callaway, L. Yano, and K. Herzig, "The effect of d-amphetamine, clonidine, and yohimbine on human information processing," *Psychophysiology*, no. 31, pp. 331–337, 1994.

[4] M. Lindgren, L. Molander, C. Verbaan, E. Lunell, and I. Rosén, "Electroencephalographic effects of intravenous nicotine: A dose-response study," *Psychopharmacology*, vol. 145, pp. 342–350, 1999.

[5] W. B. Pickworth, S. J. Heishman, and J. E. Henningfield, "Relationships between EEG and performance during nicotine administration and withdrawal," in *Brain Imaging of Nicotine and Tobacco Smoking*, E. F. Domino, Ed. Ann Arbor, MI: NPP, 1995, pp. 275–287.

[6] D. J. Thomson, "Spectrum estimation and harmonic analysis," *Proc. IEEE*, vol. 70, pp. 1055–1096, Sept. 1982.

[7] Y. Xu, S. Haykin, and R. J. Racine, "Multiple window time-frequency distribution and coherence of EEG using slepian sequences and hermite functions," *IEEE Trans. Biomed. Eng.*, vol. 46, pp. 861–866, July 1999.

[8] A. T. Walden, E. McCoy, and D. B. Percival, "The variance of multitaper spectrum estimates for real gaussian processes," *IEEE Trans. Signal Processing*, vol. 42, pp. 479–482, Feb. 1994.

[9] M. Hansson and G. Salomonsson, "A multiple window method for estimation of peaked spectra," *IEEE Trans. Signal Processing*, vol. 45, pp. 778–781, Mar. 1997.

[10] M. Hansson, "Optimized weighted averaging of peak matched multiple window spectrum estimates," *IEEE Trans. Signal Processing*, vol. 47, pp. 1141–1146, Apr. 1999.

Maria Hansson (S'90–M'96) was born in Sweden 1966. She received the M.S. degree in electrical engineering and the Ph.D. degree in signal processing from Lund University, Lund Sweden, in 1989 and 1996, respectively.

Her current research interests include multiple window spectrum analysis, time-varying signal processing and estimation of transient signals with application to biomedicine and acoustics.

Magnus Lindgren was born in 1961 in Kalmar, Sweden. He holds a doctorate in psychology from Lund University and is a licensed psychologist.

His main research interests concern applications of event-related potentials. He shares his time between research and clinical practice in a neuropsychiatric clinic.